WEP Warwick Evans Publishing

International Journal of Materials Science and Technology Studies

ISSN: 3006-7693 (Print), ISSN: 3006-3744 (Online) | Volume 5, Number 2, Year 2026
DOI: https://doi.org/10.62051/ijmsts.v5n2.05
Journal homepage: https://wepub.org/index.php/IJMSTS/index

Iron-Modified CTNT Fiber for Non-Enzymatic Glucose Sensing

Yiming Jin *

School of Materials and Chemistry, University of Shanghai for Science and Technology, 516 Jungong Rd, Yangpu 200093, Shanghai, China

*Corresponding Author: 2124540781@qq.com

ABSTRACT

This chapter investigates a CTNT (C/TiO_2/Ti) fiber platform modified with an iron-based active phase for non-enzymatic glucose sensing. Iron catalytic sites were introduced onto the CTNT electrode without binders to improve interfacial reaction efficiency and signal stability during glucose electro-oxidation. A conductive porous core-shell CTNT fiber electrode was first prepared by anodization and gas-phase carbonization, followed by potentiostatic electrodeposition using $FeCl_3$ to obtain Fe@CTNT. SEM/EDS was used to analyze the loading state and distribution of the iron species, and the cyclic voltammetric response, working potential, amperometric sensing performance, anti-interference behavior, cycling stability, and preparation reproducibility were systematically evaluated in 0.1 M NaOH under the same conditions as for Ni@CTNT. These results provide an experimental basis for applying iron-based systems in fiber-shaped flexible electrodes.

KEYWORDS

Iron-based active phase; CTNT fiber electrode; Electrodeposition; Non-enzymatic glucose sensing; Amperometry; Alkaline medium; Cycling stability

1. RESEARCH BACKGROUND

1.1. Enzymatic Glucose Sensors

The origin of glucose sensing did not begin with the sensor itself, but with early efforts to understand biological metabolism. At the beginning of the twentieth century, researchers recognized that glucose concentration was closely related to metabolic activity. In studies of tumor metabolism, Otto Warburg proposed that glucose reacts with oxygen and is ultimately converted into carbon dioxide and water, providing an important theoretical basis for later glucose-related detection. Rudolf Buchner and co-workers subsequently found in yeast studies that glucose can be converted into gluconic acid through enzymatic reactions, accompanied by the formation of hydrogen peroxide. Because hydrogen peroxide can be detected electrochemically, researchers began to use its signal as an indirect indicator of glucose concentration [1]. On this basis, Leland Clark and John W. Lyons proposed in 1956 an electrochemical glucose detection system based on the hydrogen peroxide generated by glucose oxidase (GOx) catalysis [2]. Subsequent studies showed that electrodes could respond effectively to hydrogen peroxide, thereby linking glucose concentration with electrochemical output. By 1958, Clark and Lyons had further immobilized glucose oxidase on the electrode surface, giving rise to an early prototype of the glucose sensor. Its basic principle is that glucose is oxidized by the enzyme to produce hydrogen peroxide, and the electrochemical signal of hydrogen peroxide is then used to determine glucose concentration. Later work gradually shifted toward enzyme immobilization, electrode selection, and stability improvement [3], which promoted the continued development of enzymatic glucose sensors over the following decades [4].

Content from this work may be used under the terms of CC BY-NC 4.0 licence (https://creativecommons.org/licenses/by-nc/4.0/). Published by Warwick Evans Publishing.

1.2. Non-Enzymatic Glucose Sensors

Enzymatic glucose sensors dominated this field for a long time. Although glucose oxidase-based systems were widely used and developed rapidly, their limitations became increasingly clear as research progressed. Enzyme activity is highly sensitive to temperature, pH, and storage conditions [5], which directly affects sensor lifetime and measurement stability. For this reason, detection strategies that do not rely on biological enzymes have attracted increasing attention. Non-enzymatic glucose sensors directly catalyze glucose oxidation through active materials on the electrode surface and convert it into measurable electrical signals [6]. Common catalytic materials include transition-metal oxides such as copper oxides and cobalt oxides, as well as metals such as silver, gold, and platinum [7]. At suitable potentials, these materials can promote glucose electro-oxidation and convert concentration changes into current signals. With the development of nanotechnology, researchers further turned their attention to metallic nanomaterials. Compared with bulk materials, nanoparticles provide larger specific surface areas and more surface active sites, and therefore usually exhibit higher catalytic efficiency. In particular, noble metals such as Au, Ag, and Pt often show markedly improved reaction rates and sensitivities at the nanoscale [8].

The introduction of metallic nanomaterials has, to some extent, overcome the activity and selectivity limitations of conventional metal catalysts [9]. Further coupling them with carbon-based materials often leads to additional performance improvements in non-enzymatic glucose sensors [10]. This is because carbon materials not only possess good electrical conductivity, but can also act synergistically with metallic active components, enabling reliable responses even in complex systems. The value of nanotechnology lies not only in expanding the range of materials, but also in enabling finer control over particle size, morphology, and surface state [11]. These structural factors in turn affect response speed, stability, and the detection limit of the sensor [12].

2. INTRODUCTION

Non-enzymatic electrochemical glucose sensors have shown promise in diabetes-assisted management, food analysis, and on-site rapid testing because they do not require enzyme immobilization, generally offer better stability, and involve relatively simple fabrication procedures. However, several key issues still need to be addressed before these systems can be used more broadly in practice. First, poor dispersion and adhesion of active components on the electrode surface can lead to agglomeration or detachment, thereby limiting the number of accessible reaction sites. Second, conventional drop-casting or coating methods usually rely on polymer binders, which may block catalytic sites and introduce additional interfacial resistance, thus weakening charge transfer and response kinetics. These problems are often even more pronounced in fiber-shaped flexible electrodes because of their limited dimensions and possible bending during use. Therefore, constructing a binder-free, integrated electrode architecture with both good conductivity and mechanical stability is an important prerequisite for improving non-enzymatic glucose sensing performance.

Carbon-coated TiO_2 nanotube fiber electrodes (CTNT) provide a suitable platform for addressing these issues. This structure consists of TiO_2 nanotube arrays grown in situ on a titanium wire surface, featuring ordered channels and a large specific surface area that can supply abundant loading sites while facilitating electrolyte wetting and mass transport. Meanwhile, the outer conductive carbon layer effectively compensates for the intrinsically poor conductivity of TiO_2 by establishing continuous electron-transport pathways throughout the nanotube framework, thereby reducing charge-transfer resistance and accelerating the electrochemical response. More importantly, CTNT is tightly integrated with the metallic substrate and maintains good overall structural stability, making it naturally suitable for fiber-shaped flexible electrode systems and providing a reliable basis for the subsequent introduction of transition-metal active phases.

Among various transition metals, iron-based materials have attracted sustained interest in electrocatalysis and sensing because of their natural abundance, low cost, low environmental burden, and flexible valence-state conversion. In alkaline media, electrodeposited iron species commonly exist in the form of iron oxides/oxyhydroxides and can participate in catalytic reactions through Fe^{2+}/Fe^{3+}-related surface redox processes. In addition, the adsorption and activation of OH^- at iron-based sites, together with interfacial charge coupling between the iron species and conductive carbon, may jointly promote interfacial glucose electro-oxidation. Based on this rationale, directly coupling an iron-based active phase to the CTNT conductive framework without using polymer binders is expected to improve the utilization of active sites while also delivering more stable current output, thus offering a feasible route for flexible fiber-shaped non-enzymatic glucose sensing.

Following this strategy, $FeCl_3$ was used in this chapter as the precursor to construct Fe@CTNT fiber-shaped electrodes on CTNT fiber substrates by electrodeposition, and their structure and electrochemical behavior were investigated under the same conditions as those used for the Ni@CTNT system (for example, in 0.1 M NaOH). By combining SEM/EDS, Raman, and XPS characterization, the morphology, distribution, and valence features of the iron-based active phase were analyzed. CV, EIS, and i-t measurements were further employed to evaluate glucose sensing performance, including sensitivity, linear range, detection limit, response time, anti-interference capability, reproducibility, and stability, and to discuss the feasibility of practical sample analysis.

3. PREPARATION OF SENSOR ELECTRODES

3.1. Preparation of the CTNT Electrode

The CTNT fiber electrode was prepared by a combination of anodization and chemical vapor deposition. A titanium wire with a length of about 7 cm was first used as the substrate, ultrasonically cleaned in ethanol, acetone, and ethanol in sequence, and the cleaning procedure was repeated twice in a fume hood to remove surface oil and impurities, after which the wire was naturally dried. The titanium wire was then used as the working electrode and a platinum sheet as the counter electrode, and anodization was carried out at 25 °C in 0.3 M NH_4F electrolyte under a constant voltage of 60 V for 5.5 h. This treatment produced a relatively ordered TiO_2 nanotube array grown in situ on the titanium wire surface, yielding a Ti/TiO_2 bilayer structure.

The Ti/TiO_2 bilayer was then placed in a tube furnace for carbonization. The sample was first pretreated in air, then heated to 800 °C under Ar protection while a mixed gas of H_2 and C_2H_2 was introduced and maintained for 1 h, allowing a conductive carbon layer to form on the surface of the TiO_2 nanotubes. After the reaction, the gas flow was stopped and the sample was naturally cooled to room temperature under Ar, finally yielding a CTNT fiber composite electrode with a $C/TiO_2/Ti$ multilayer core-shell structure.

3.2. Preparation of the Fe@CTNT Electrode

Ferric chloride hexahydrate was dissolved in deionized water to prepare a 40 mM precursor solution and diluted to a final volume of 100 mL, followed by thorough stirring until the solution became completely clear. The prepared CTNT fiber electrode was then immersed in the $FeCl_3$ solution and potentiostatic electrodeposition was carried out in a three-electrode system, with CTNT as the working electrode, a platinum sheet as the counter electrode, and Ag/AgCl as the reference electrode. Iron-based species were deposited at -1.5 V to obtain the Fe@CTNT fiber-shaped electrode. After deposition, the electrode was gently rinsed with deionized water to remove residual salts and then dried at 80 °C for later use.

4. MORPHOLOGICAL AND STRUCTURAL CHARACTERIZATION OF THE ELECTRODES

4.1. SEM and TEM Morphological Characterization

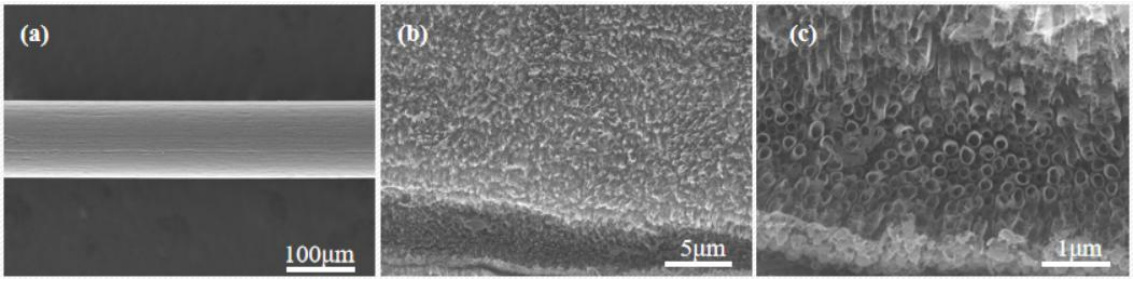

Figure 1. SEM images of the TiO_2 surface at different magnifications

The surface morphology of the samples was observed by field-emission scanning electron microscopy (FESEM). As shown in Figure 1, anodization generated a relatively ordered TiO_2 nanotube array on the titanium wire surface, with clearly visible tube openings and a fairly uniform pore-size distribution. This ordered one-dimensional nanotubular structure can enlarge the effective surface area of the electrode and provide stable support for subsequent carbon growth and iron-based active-phase loading, which is beneficial for constructing a composite electrochemical reaction interface.

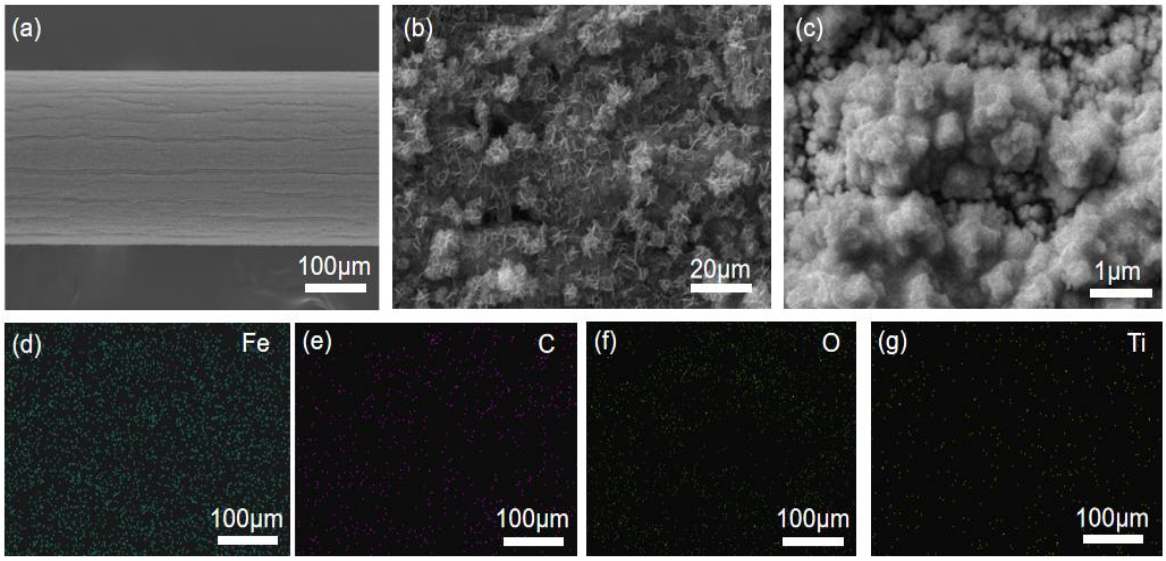

Figure 2. SEM images of the Fe-loaded sample at different magnifications: (a-c) morphology under different resolutions; elemental mapping of (d) Fe, (e) C, (f) O, and (g) Ti

As shown in Figure 2(a), the Fe@CTNT fiber electrode still maintains a continuous and relatively uniform fibrous morphology, and the surface coating remains basically intact. This indicates that electrodeposition enabled the iron-based species to form a continuous deposited layer or particulate covering on the titanium wire/CTNT substrate. Such a coverage state helps preserve structural integrity under bending or long-term immersion and also provides a relatively stable interface for subsequent electrochemical reactions.

At a medium magnification (Figure 2(b)), the electrode surface exhibits obvious rough and porous characteristics, showing flocculent or network-like features formed by the stacking of fine nanostructures. Such rough porous surfaces usually imply a larger effective surface area and more accessible active sites. At the same time, the pore network facilitates rapid electrolyte penetration and

ion diffusion, thereby reducing mass-transfer resistance and improving the current response rate. This type of surface structure is generally favorable for non-enzymatic glucose detection.

At higher magnification (Figure 2(c)), the surface can be seen to consist mainly of numerous nanoparticles or clusters at the nanoscale, with a certain degree of aggregation, overall appearing as particle-like clusters attached to the framework surface. This morphology is consistent with the $FeCl_3$ aqueous electrodeposition system, indicating that the iron-based species tend to form iron oxides/oxyhydroxides or amorphous/poorly crystalline clusters during deposition and subsequent exposure. Moderate aggregation is beneficial for forming continuous conductive contact, but an excessively thick deposited layer may block some pores and reduce electrolyte accessibility.

EDS results (Figure 2(d-g)) show that Fe@CTNT is mainly composed of Fe, C, O, and Ti. Among these elements, Fe is distributed continuously and relatively uniformly over a large area, without obvious local enrichment or blank regions, indicating that the iron-based deposited phase can be loaded rather uniformly on the CTNT surface. Such uniformity is important for sensors because it helps reduce local current hot spots, allowing active sites to participate in the reaction more consistently and thereby improving signal stability while reducing electrode-to-electrode variation.

At the same time, C covers the entire analyzed region, consistent with the carbon-coating feature of CTNT, whereas Ti and O correspond to the underlying TiO_2/titanium-wire framework, indicating that the substrate structure remains intact after the introduction of the iron-based species. It should be noted that EDS can only provide semi-quantitative information on elemental composition and spatial distribution and cannot directly determine chemical purity or valence states with high precision. Nevertheless, no obvious enrichment of other impurity elements was observed within the detectable range, and the continuous distribution of Fe further supports the successful construction of the Fe@CTNT composite structure.

Taken together, the SEM and EDS results indicate that the Fe@CTNT electrode surface is covered by a rough and porous layer composed of iron-based nanoparticles/clusters, while Fe remains relatively uniformly distributed on the macroscopic scale. This structure not only increases the effective surface area and the number of accessible active sites, but also relies on the CTNT conductive framework to establish continuous charge-transport pathways, and is therefore expected to improve both interfacial charge transfer and reaction kinetics. Another point worth noting is that a relatively uniform loading layer can help reduce local signal drift and hot-spot effects, thereby improving consistency among electrodes and providing a favorable structural basis for subsequent sensing-performance evaluation.

5. ELECTROCHEMICAL PERFORMANCE CHARACTERIZATION OF THE ELECTRODES

5.1. Electrochemical Characterization of the Fe@CTNT Electrode

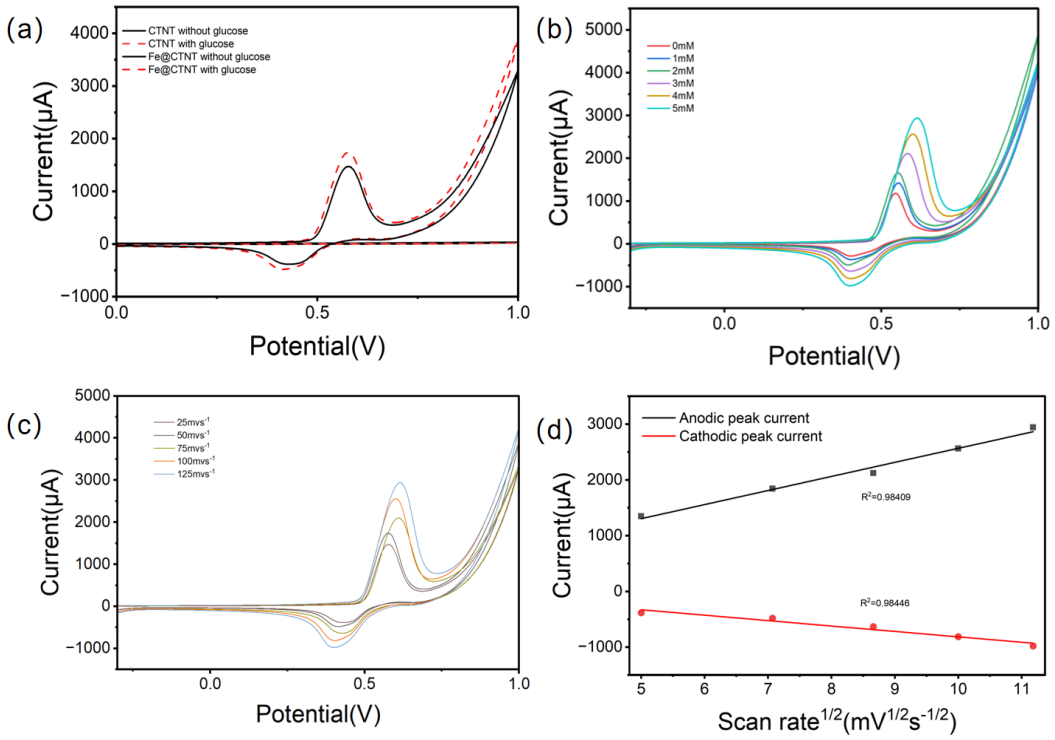

Figure 3. (a) Cyclic voltammograms of a bare titanium-wire electrode and an Fe@CTNT electrode in 0.1 M NaOH with and without 1 mM glucose; (b) cyclic voltammograms of the Fe@CTNT electrode in 0.1 M NaOH with different glucose concentrations; (c) cyclic voltammograms of the Fe@CTNT electrode in 0.1 M NaOH at different scan rates (25-125 mV s^{-1}); (d) linear fits of the anodic and cathodic peak currents versus the square root of scan rate

Figure 3(a) compares the bare titanium wire and the Fe@CTNT electrode, showing that the glucose response mainly originates from interfacial electrocatalysis after the introduction of the iron-based active phase. The voltammogram of bare titanium wire changes very little before and after glucose addition, whereas the anodic current of Fe@CTNT increases markedly in the presence of glucose, indicating that this electrode can effectively promote glucose electro-oxidation under alkaline conditions. As seen in Figure 3(b), the oxidation-related current increases continuously with increasing glucose concentration, demonstrating a clear concentration-dependent response that is suitable for subsequent quantitative analysis. The scan-rate results in Figure 3(c) show that the peak current increases with increasing scan rate, accompanied by slight peak shifts, suggesting the existence of polarization and kinetic limitations. Furthermore, the good linear relationship between peak current and $v^{1/2}$ in Figure 3(d) indicates that the process is mainly diffusion-controlled, meaning that mass transport of glucose from the bulk solution to the electrode surface plays an important role in the overall reaction rate. This behavior is consistent with that commonly observed in non-enzymatic glucose oxidation systems and also provides a basis for later amperometric measurements.

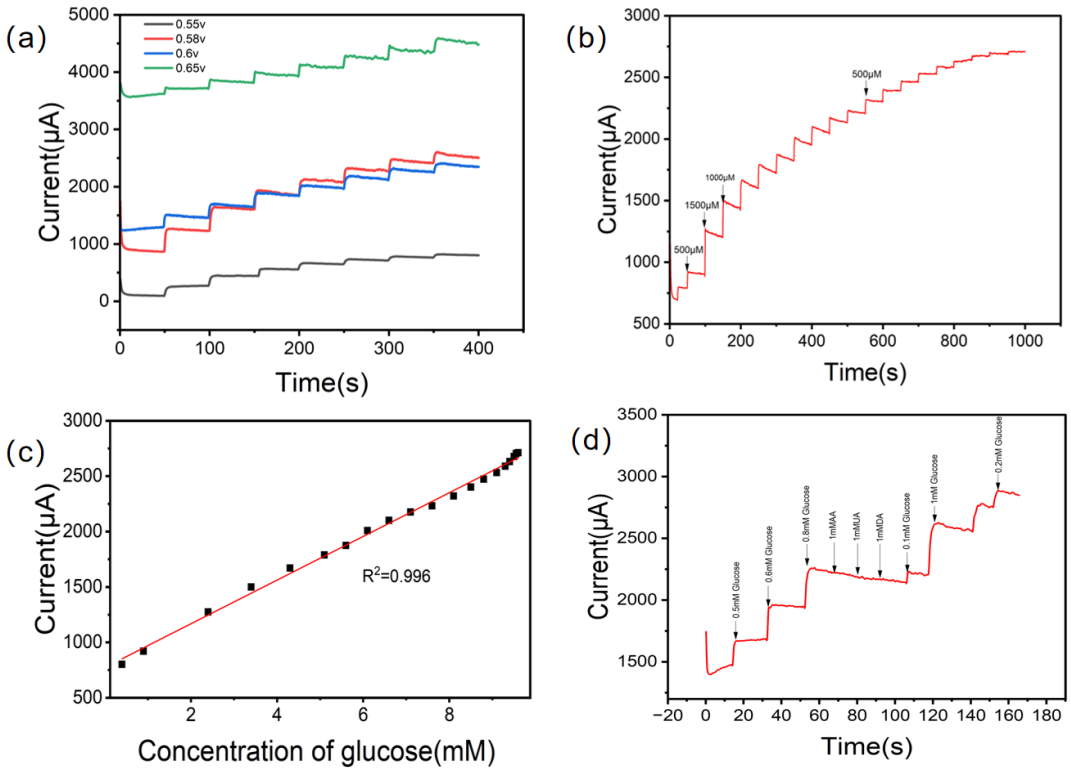

Figure 4. (a) Current-time curves recorded in 0.1 M NaOH at different applied potentials (0.55-0.65 V) with seven successive additions of 0.5 mM glucose at 50 s intervals; (b) current-time response at 0.65 V in 0.1 M NaOH upon successive additions of glucose at different concentrations; (c) linear fit between the response current and glucose concentration in alkaline solution; (d) current-time curves obtained after successive addition of glucose, AA (ascorbic acid), UA (uric acid), and DA (dopamine) in 0.1 M NaOH

The choice of working potential directly affects response intensity, background current, and anti-interference performance. Figure 4(a) compares the stepwise current responses obtained during continuous addition in the range of 0.55-0.65 V. In general, when the potential is too low, the catalytic driving force is insufficient and the current response is weak; when the potential is too high, larger background currents and side reactions may occur, leading to greater signal fluctuation. Considering both response amplitude and baseline stability, 0.65 V was selected as the working potential in this chapter. Under this condition, Figure 4(b) shows that Fe@CTNT can produce rapid and reproducible stepwise current responses toward different glucose concentrations and can reach a stable state within a short time, indicating fast interfacial reaction kinetics. The calibration curve in Figure 4(c) demonstrates a good linear relationship between steady-state current and glucose concentration within the investigated range, satisfying the requirement for quantitative detection. If deviation from linearity appears at higher concentrations, it is usually associated with gradual saturation of active sites, thickening of the diffusion layer, or limited local OH^- supply. The anti-interference test in Figure 4(d) further shows that the current changes induced by AA, UA, and DA are much smaller than those caused by glucose, indicating that the system possesses a certain degree of selectivity and resistance to matrix interference under the chosen operating conditions.

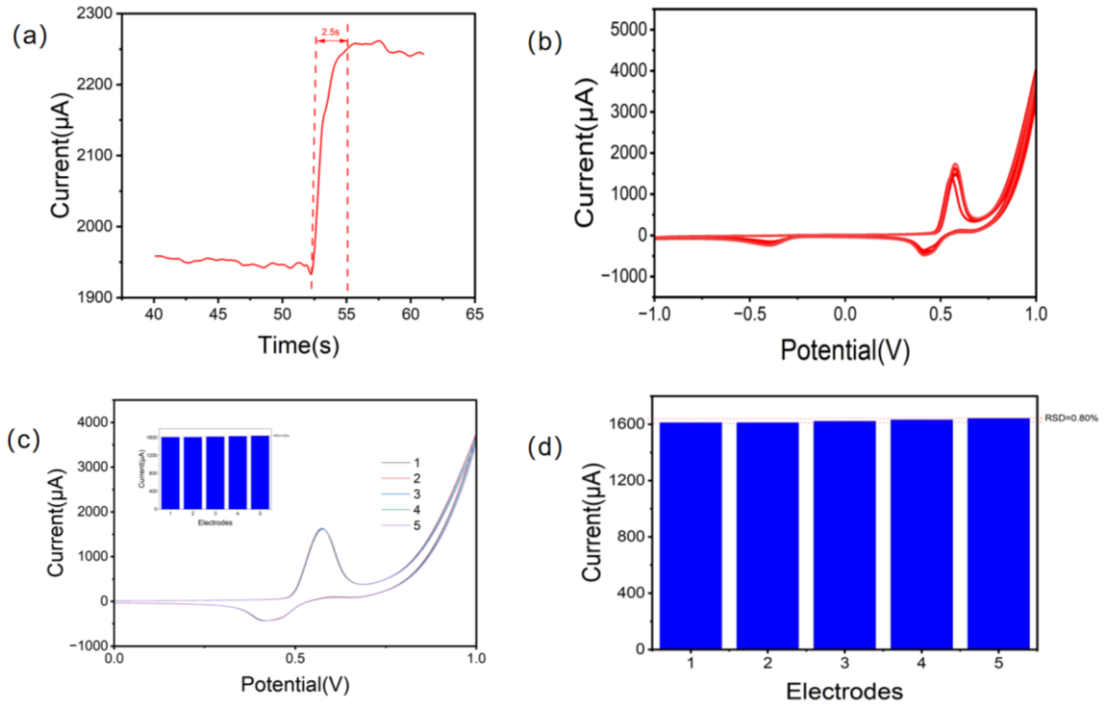

Figure 5. (a) Response time of the Fe@CTNT electrode in 0.1 M NaOH containing 1 mM glucose; (b) cyclic voltammograms of the Fe@CTNT electrode after 20 consecutive scans in 0.1 M NaOH containing 1 mM glucose; (c) response current values of five Fe@CTNT electrodes under identical experimental conditions; (d) RSD of the five response current values

To assess the reliability of this electrode in practical use, its response speed, cycling stability, and preparation reproducibility were further evaluated. Figure 5(a) reflects the time required for the current to reach a steady state after analyte addition. A faster response usually indicates smoother charge transfer and mass transport, which is consistent with the porous channels and continuous conductive network provided by the CTNT structure. If the 20 consecutive CV curves in Figure 5(b) remain largely overlapped, or if the peak-current decay is small, it indicates that the iron-based active phase has good stability and adhesion within this testing window. Meanwhile, Figure 5(c-d) summarizes the response currents of five independently prepared electrodes and presents the corresponding RSD values. A small RSD indicates low batch-to-batch variation and good process reproducibility, suggesting that this method has a sound basis for further practical sample analysis. Overall, Fe@CTNT maintains a strong glucose response while also exhibiting good stability and reproducibility.

6. CONCLUSION

Using a CTNT fiber-shaped conductive electrode as the platform, an iron-based active phase was introduced onto the nanotube framework by electrodeposition from an $FeCl_3$ solution, and a Fe@CTNT fiber-shaped non-enzymatic glucose sensing electrode was successfully prepared. SEM and EDS results show that the deposited iron-based species form a relatively continuous and uniformly distributed nanostructured coating on the CTNT surface, while the original porous characteristics of the substrate are largely retained. This preserves channels for electrolyte wetting and mass transport and also provides a structural basis for output consistency and batch-to-batch reproducibility.

Electrochemical tests demonstrate that Fe@CTNT shows a clear response toward glucose oxidation in alkaline medium. Comparative CV experiments indicate that the enhanced current signal arises from the introduction of the iron-based active phase, while concentration-dependent CV results and

scan-rate analysis show that the system possesses relatively clear kinetic characteristics that support quantitative detection. After optimization of the working potential and amperometric i-t testing, Fe@CTNT exhibits stable and rapid stepwise responses and establishes a good current-concentration relationship, demonstrating its potential for non-enzymatic quantitative glucose sensing.

In addition, the anti-interference experiments show that Fe@CTNT can effectively suppress the influence of common interferents such as AA, UA, and DA. The cycling-stability and multi-electrode reproducibility results also indicate that the electrode can maintain relatively stable electrochemical behavior during continuous operation and that the preparation method has good repeatability. Overall, coupling the iron-based active phase with the CTNT conductive framework enables this fiber-shaped platform to achieve a favorable balance among active-site accessibility, electron-transport efficiency, and structural stability, thereby realizing rapid, stable, and reproducible non-enzymatic glucose detection. The results presented in this chapter provide a useful experimental reference for the further construction and application of iron-based active phases on CTNT platforms.

REFERENCES

[1] Panditharatne S P, Imali D Y, Perera E C J, et al. Anodized CuO-based reusable non-enzymatic glucose sensor as an alternative method for the analysis of pharmaceutical glucose infusions: a cyclic voltammetric approach [J]. Analytical Sciences, 2024, 40: 1475–1487.

[2] Updike S, Hicks G. The enzyme electrode [J]. Nature, 1967, 214(5092): 986–988.

[3] Kondee S, Pon-On W, Siriwatcharapiboon W, et al. CuO/SnS_2 nanoparticles on PEDOT: PSS for nonenzymatic electrochemical glucose sensors [J]. ACS Applied Nano Materials, 2024, 7(6): 6722–6735.

[4] Emin A, Ding A, Ali S, et al. Electrochemical non-enzymatic glucose biosensors based on Au-thiol-linked molecular architectures [J]. Microchemical Journal, 2024, 190: 111972.

[5] Dao Q K, Mai T Q, Pham T V, et al. ZnO nanorods grown on Cu wire mesh provide a high sensitivity non-enzymatic absorbance glucose sensor [J]. Microchimica Acta, 2024, 191: 753.

[6] Filimonenkov I S, Urvanov S A, Kurzhumbaev D Z, et al. Three kinds of Pt electrocatalysts for the non-enzymatic glucose sensing in a neutral medium [J]. Journal of Applied Electrochemistry, 2025.

[7] Zhang H, Yin J, Wang Y, et al. NiO-decorated cocoon silk-derived carbon-based non-invasive electrochemical sensor for detecting glucose in saliva [J]. Journal of Materials Science, 2024, 59: 21868–21881.

[8] Gopal T S, James J T, Gunaseelan B, et al. MXene-embedded porous carbon-based Cu_2O nanocomposites for non-enzymatic glucose sensors [J]. ACS Omega, 2024, 9(7): 8448–8456.

[9] Liao L, Xu F, Sun L, et al. Fabrication of a novel non-enzymatic glucose sensor based on ruthenium supported by a combination of PBA nanocubes and MOF nanosheets [J]. Microchemical Journal, 2024, 207: 111791.

[10] Afruz A, Amiri M, Kaffash-Jamshid M, et al. Dual-function nickel bio-MOF as a non-enzymatic glucose sensor and efficient supercapacitor [J]. Electrochimica Acta, 2025, 513: 145586.

[11] Yaseen J, Saira F, Imran M, et al. Synthesis of CuSe/PVP/GO and CuSe/MWCNTs for their applications as nonenzymatic electrochemical glucose biosensors [J]. RSC Advances, 2024, 14: 6896–6905.

[12] Zhou F, Wang J, Tang Y, et al. Enhanced sensing performance of flexible non-enzymatic electrochemical glucose sensors using hollow Fe_3O_4 nanospheres of controllable morphologies [J]. Ceramics International, 2024, 50(20, Part A): 38009–38021.